

## Quantitative Structure – Pharmacokinetic Relationships for Plasma Clearance of Basic Drugs with Consideration of the Major Elimination Pathway

Zvetanka Zhivkova

Faculty of Pharmacy, Medical University of Sofia, Sofia 1000, Bulgaria.

Received, April 7, 2017; Revised, May 3, 2-17; Accepted, May 16, 2017; Published, May 16, 2017.

**ABSTRACT: Purpose.** The success of a new drug candidate is determined not only by its efficacy and safety, but also by proper pharmacokinetic behavior. The early prediction of pharmacokinetic parameters could save time and resources and accelerate drug development process. Plasma clearance (CL) is one of the key determinants of drug dosing regimen. The aim of the study is development of quantitative structure – pharmacokinetics relationships (QSPkRs) for the CL. **Methods.** A dataset consisted of 263 basic drugs, which chemical structures were described by 154 descriptors. Genetic algorithm, stepwise regression and multiple linear regression were used for variable selection and model development. Predictive ability of the models was assessed by internal and external validation. **Results.** A number of significant QSPkR models for the CL were derived with respect to the primary elimination pathway (renal excretion, metabolism, or CYP3A4 mediated biotransformation), as well for the unbound clearance ( $CL_u$ ). The models were able to predict 52 – 80% of the drugs from external validation sets within the 2-fold error of the experimental values with geometric mean fold error 1.57 – 2.00. **Conclusions.** Plasma protein binding was the major restrictive factor for the CL of drugs, primarily cleared by metabolism. The clearance was favored by lipophilicity and several structural features like OH-groups, aromatic rings, large hydrophobic centers, aliphatic groups, connected with electro-negative atoms, and non-substituted aromatic C-atoms. The presence of Cl-atoms and abundance of 6-member aromatic rings or fused rings had negative effect. The presence of ether O-atoms contributed negatively to the CL of both metabolism and renally excreted drugs, and urine excretion was favored by the presence of 3-valence N-atoms. These findings give insight on the main structural features governing plasma CL of basic drugs and could serve as a guide for lead optimization in the drug development process.

This article is open to **POST-PUBLICATION REVIEW**. Registered readers (see “For Readers”) may **comment** by clicking on ABSTRACT on the issue’s contents page.

### INTRODUCTION

Drug discovery and development is an expensive and time consuming process. Many promising drug candidates with appreciable activity *in vitro* fail to become marketable products because of lack of efficacy *in vivo*, most often due to inappropriate pharmacokinetic behavior. The early prediction of ADME (absorption, distribution, metabolism and excretion) is of paramount importance for saving time and resources and for increasing the success of new drug candidates. Thanks to the extensive research on the prediction of key ADME parameters the percentage of drug development failures due to pharmacokinetic and bioavailability problems dropped markedly from 40% in 1991 to 10% in 2000 (1).

In the last two decades computational (*in silico*) modeling becomes a powerful tool for ADME prediction (2 – 6). It enables development of quantitative structure – pharmacokinetics relationships (QSPkRs) based on molecular structure and physicochemical descriptors. QSPkRs allow predictions of ADME even of virtual compounds, thus accelerating identification of new drug candidates and reducing the cost of drug development process. In addition, they give insight into the most important structural features governing pharmacokinetic behavior.

---

**Corresponding Author:** Dr. Zvetanka Zhivkova; Associate Professor; Faculty of Pharmacy, Medical University of Sofia; 2 Dunav st., 1000 Sofia, Bulgaria; Email: zdzhivkova@yahoo.com

Human plasma clearance (CL) is one of the most important ADME parameters. It is a proportionality coefficient between the rate of elimination and plasma concentration. It determines drug half-life (together with the steady state volume of distribution,  $V^{ss}$ ) and bioavailability (together with trans-membrane permeability) and consequently is the major decisive factor in setting up reliable dosage regimen (7).

Several reports on QSPkR modeling of drug CL have been published recently. A wide suite of statistical and machine learning methods were used: multiple linear and non-linear regression analysis (3), partial least squares (4 – 12), artificial neural networks (13), k-nearest neighbor (9, 10, 14), general regression network and support vector regression (10). The models show satisfactory predictive ability, but some of them are not well validated, and another do not offer sufficient interpretability. Therefore, a well-constructed, well-validated and interpretable QSPkR model would still be relevant.

*In silico* prediction of drug CL is a difficult task because of the complexity of the elimination process involving a sequence of diverse processes (renal and hepatic uptake, metabolism, glomerular filtration, tubular secretion and reabsorption, bile excretion, etc.), each with specific structural requirements. Knowledge on the elimination mechanisms could improve CL prediction, but for the majority of the drugs the available information is rather insufficient. Successive drug CL modeling is further complicated by plasma protein binding (PPB) which is often a restrictive factor for drug clearance. Alternatively, QSPkR models could be derived for the unbound clearance  $CL_u$ . This is the clearance of the unbound drug in plasma, which can be considered as independent of PPB and affected solely by the chemical structure.

The published so far QSPkR models for drug CL are built either on limited congeneric series, or on large datasets involving molecules of all charged types. It is well established that acidic and basic drugs follow different pharmacokinetic patterns. Acids have considerably lower  $V^{ss}$  (15). They bind preferably to human serum albumin (HSA) in plasma, and the ionization at physiological pH 7.4 hinders their distribution in tissues. In contrast, bases are bound mainly to alpha-1-acid glycoprotein, have high affinity to membrane phospholipids and can be accumulated by ion-trapping into lysosomes (15). The CL of acids is also lower than those of bases.

According to a published analysis of a large dataset of 754 compounds, majority of compounds belonging to anionic (78%) and zwitter-ionic (80%) class have low CL, and only 1-2% – high. On contrary, only 29% of the cationic compounds showed low CL (11). Acidic drugs seem to be more often subjected to renal and biliary excretion, while metabolism is the primary clearance mechanism for bases. Specific transporters enable drug uptake into kidney and bile – organic anion transporters for acids, and organic cation transporters – for bases (16). Different enzymes are also involved in the metabolism. For example, in terms of CytP450 oxidation, anionic drugs are preferred substrates of CYP2C9, while most of the basic drugs are metabolized either by CYP2C19 or CYP3A4 (17). Therefore, construction of separate QSPkRs according to the ionization state of the molecules seems to be more reliable.

Recently we published a series of reports on *in silico* prediction of several ADME parameters of acids (18 – 21) and bases (22). The aim of the present study is: 1. Development of QSPkRs for total plasma CL and  $CL_u$  of basic drugs; 2. Generation of separate QSPkRs for the CL of basic drugs, eliminated primarily by renal excretion or by metabolism. 3. Identification of the main structural features governing plasma CL of basic drugs.

## METHODS

### Datasets

The drugs used in the present study were extracted from the original work of Obach et al. (23) providing data for the major pharmacokinetic parameters of 659 drugs after *iv* administration in human. A drug was considered as a base in two occasions: 1. If the fraction ionized as a base ( $f_B$ ) at pH 7.4 exceeded 3%, and 2. If the molecule possessed any acidic group, but  $f_B$  was considerably higher than the fraction ionized as an acid ( $f_A$ ). The  $f_A$  and  $f_B$  fractions were calculated according to equations:

$$f_A = \frac{1}{1 + 10^{(pK_a - 7.4)}} \quad (1)$$

$$f_B = \frac{1}{1 + 10^{(7.4 - pK_a)}} \quad (2)$$

In the case of more than one ionizable group, the strongest one was taken into account. The  $pK_a$  values were calculated with ACD/logD version 9.08

software (Advanced Chemistry Development Inc., Ontario, Canada).

266 drugs were eligible to be considered as bases. Three of them were excluded from the dataset: methylphenidate – because of the highly contradicting literature data for its CL, epirubicin – epimer of doxorubicin, and dilevalol – R-isomer of labetalol. The final dataset consisted of 263 molecules. On the basis of extensive literature search the drugs were classified according to their primary elimination path. Drugs were considered as renally cleared if the fraction excreted unchanged in urine exceeded 60% and no data for significant non-renal excretion were found; 40 drugs met this criteria. Another 180 drugs with a fraction eliminated by metabolism exceeding 70% were assigned as metabolically cleared. Only 6 drugs were identified as biliary cleared. For 17 compounds no reliable information regarding clearance mechanism was found. Finally, 20 drug drugs appeared to have mixed clearance mechanism – almost 50:50 of any two of the classes. More detailed information about the dataset is given in the Supplementary file.

The mol-files of the drugs were taken from several public databases: Drug Bank (24), Chemical Book (25) or Japan Chemical Compounds Dictionary (26). The values for the total clearance CL and the unbound fraction in plasma  $f_u$  were taken from Obach's database. The end-point variable was presented as logCL or logCL<sub>u</sub> in order to achieve close to normal distribution.

Several datasets were generated, including: all drugs (n=263), drugs with available data for  $f_u$  (n=220), renally cleared drugs (n=40), drugs cleared primarily by metabolism (n=180), drugs cleared by CYP3A4 mediated metabolism (n=87), etc. In most cases the original datasets were divided into training and external test set for model validation. To this end the molecules were arranged in an ascending order according to their CL or CL<sub>u</sub> value, and one of the every four or five drugs (depending on the number of the compounds) was allocated to a different subset. One of the subsets was excluded as an external test set, and the remaining three (four) composed the training set.

### Molecular descriptors and variable selection

The chemical structures of the compounds were described by 154 molecular descriptors calculated by ACD/logD version 9.08 (Advanced Chemical Development, Inc.) and MDL QSAR version 2.2 (MDL Information Systems Inc., San Leandro, CA).

The descriptors included electrotopological and molecular connectivity indices, descriptive properties (number of specific atoms and groups, rings, circles, hydrogen bond donors and acceptors), whole molecular features (molecular weight, logP, logD<sub>7.4</sub>, dipole moment, volume, surface, etc.). The most significant descriptors were selected in a three step procedure. First – for each training set, descriptors with non-zero values for less than five molecules were rejected. The remaining descriptors were filtered through genetic algorithm (GA). Finally, the selected descriptors entered a forward stepwise linear regression (SWR) with Fisher criteria F-to-enter 4.00 and F-to-remove 3.99. Both GA and SWR were implemented in the MDL QSAR package.

### Generation and validation of the QSPkR models

The QSPkR models were generated by multiple linear regression (MLR). Drugs, which end-point values were predicted with residuals not obeying the normal distribution law were considered as outliers. They were removed from the training sets and the models were rebuilt. The models were assessed by the explained variance  $r^2$  given by the equation:

$$r^2 = 1 - \frac{\sum_{i=1}^n (\log Y_{i,obs} - \log Y_{i,calc})^2}{\sum_{i=1}^n (\log Y_{i,obs} - \log \bar{Y}_{obs})^2} \quad (3)$$

where  $Y_{i,obs}$  and  $Y_{i,calc}$  are the observed and calculated by the model values of CL or CL<sub>u</sub> for the  $i^{\text{th}}$  drug in the training set, and  $\bar{Y}_{obs}$  – the mean observed value, respectively.

The generated QSPkR models were validated by leave-one-out cross validation (LOO-CV) and external validation. The model performance was evaluated by the cross-validated coefficient for the training set  $q_{LOO-CV}^2$ , prediction coefficient for the external test set  $r_{pred}^2$  and geometric mean fold error of prediction GMFEP, calculated as follows:

$$q_{LOO-CV}^2 = 1 - \frac{\sum_{i=1}^n (\log Y_{i,obs} - \log Y_{i,pred})_{train}^2}{\sum_{i=1}^n (\log Y_{i,obs} - \log \bar{Y}_{obs})_{train}^2} \quad (4)$$

$$r_{\text{pred}}^2 = 1 - \frac{\sum_{i=1}^n (\log Y_{i,\text{obs}} - \log Y_{i,\text{pred}})_{\text{test}}^2}{\sum_{i=1}^n (\log Y_{i,\text{obs}} - \log \bar{Y}_{\text{obs}})_{\text{test}}^2} \quad (5)$$

$$\text{GMFEP} = 10^{\frac{\sum_{i=1}^n |\log Y_{i,\text{obs}} - \log Y_{i,\text{pred}}|}{n}} \quad (6)$$

where  $Y_{i,\text{obs}}$  and  $Y_{i,\text{pred}}$  are the observed and predicted by the model values of CL or  $\text{CL}_u$  for the  $i^{\text{th}}$  drug in the training or test set, and  $\bar{Y}_{\text{obs}}$  – the mean observed value, respectively. Accuracy of prediction was assessed as a percentage of drugs in the external test set, predicted with less than two- or three-fold error of the observed value. The fold error FE is calculated by the formula:

$$\text{FE} = 10^{|\log Y_{i,\text{obs}} - \log Y_{i,\text{pred}}|} \quad (7)$$

There are not standardized criteria for the acceptance of QSPkR models. Taking into account, that QSPkR is an extension of QSAR for ADME prediction, it is reasonable to use the accepted criteria for QSAR models. They are described in detail in several articles and summarized recently by Roy et al. (27).

The thresholds values for internal and external validation are set as follows:  $q^2 > 0.5$  and  $r_{\text{pred}}^2 > 0.5$ . However, QSPkR modeling of ADME parameters meets much more difficulties compared to the classical QSAR mainly due to the complexity of the underlying biological processes and the limited quality and quantity of experimental data. Frequently the derived QSPkR models do not satisfy above mentioned statistical criteria, and the authors report only the mean fold error of prediction MFEP, mean absolute error MAE, or geometric mean fold error of prediction GMFEP. Accuracy is usually expressed as a fraction of the molecules which PhK parameter is predicted within the two fold error of the experimental values. A two-fold error limit seems reasonable, as the values of the ADME parameters may vary considerably due to different reasons, primarily to inter-individual differences. Models with GFFEP within 2 and accuracy  $\sim 60\%$  are considered as good predictive models (11). Therefore, we also accepted the thresholds  $q_{\text{LOO-CV}}^2 > 0.5$ ,  $r_{\text{pred}}^2 > 0.5$ ,  $\text{GFFEP} \leq 2$  and accuracy  $\sim 60\%$  to evaluate the predictive ability of our QSPkR models for CL and  $\text{CL}_u$  of basic drugs.

## RESULTS

The initial attempts to derive QSPkRs for the whole dataset of 263 basic drugs failed to find any correlation between logCL and the large variety of molecular descriptors used. Since drug CL depends crucially on both clearance mechanism and PPB, further studies were continued in two ways: deriving QSPkR models for logCL with respect to the primary elimination pathway, and deriving QSPkR models for log $\text{CL}_u$ . The datasets used for QSPkR models development, together with the observed and predicted values of CL and  $\text{CL}_u$  are given in the **Supplementary file**.

### QSPkR models for the clearance of renally excreted drugs.

After a thorough literature search, 40 drugs were considered as eliminated primarily by renal excretion. The values of their CL varied between 0.55 and 3 ml/min/kg. The dataset was divided into a training set and external test set as described in **Methods**. Several models were derived using different combination of descriptors, and the best one in terms of statistics is given as Model 1: - **PLEASE SEE BELOW for Model 1**.

Two drugs (ethambutol and sotalol) were identified as outliers, although their CL values were calculated with a FE of 2.36 and 2.11, respectively. According to Model 1, the CL of renally cleared drugs is determined by three electro-topological indices, which explain about 89% of the variance. SssO encodes the number of the ether -O-atoms. SdsN signifies the presence of N-atoms, connected with a simple and a double bond to C-atoms (=N-). SsssN-account equals the number of tertiary N-atoms (>N-) in the molecule. SdsN and SsssN-account affect positively drug CL, while SssO has a negative effect. The effect of PPB on the CL of renally excreted drugs was not evaluated because of the lack of PPB data for 6 of the 40 drugs. In general, only 5 of the drugs showed PPB  $> 50\%$  ( $f_u < 0.5$ ), and no one - high PPB ( $> 90\%$ ,  $f_u < 0.10$ ). Therefore, PPB seems not to be a restrictive factor for renally cleared drugs.

Validation with the external test set of 10 molecules showed predictive correlation coefficient  $r_{\text{pred}}^2$  0.733. The model was able to predict the CL of the drugs in the external test set with GMFEP 1.57 with accuracy of 80% (at two-fold error level) and 100% (at 3-fold error level).

**Model 1.**

$$\log CL = -0.026(\pm 0.003)S_{ssO} + 0.082(\pm 0.022)S_{dsN} + 0.157(\pm 0.063)S_{sssN\_acct} + 0.626$$

n 28                      r<sup>2</sup> 0.890                      q<sup>2</sup><sub>LOO-CV</sub> 0.853                      F 64.78

The plot of the predicted by Model 1 versus observed values of logCL is presented in Figure 1.

The slope of the regression line for the training set is close to 1, and the intercept is nearly 0. This, together with the values of r<sup>2</sup> (for the training set) and r<sup>2</sup><sub>pred</sub> (for the test set), confirms the good correlation between logCL<sub>pred</sub> and logCL<sub>obs</sub>.

### QSPkR for drugs cleared primarily by metabolism

180 drugs were identified as cleared primarily by metabolism. The derived QSPkR model for logCL was unsatisfactory in terms of statistics (r<sup>2</sup> 0.356, q<sup>2</sup><sub>LOO-CV</sub> 0.289), although GMFEP was 1.78 and the accuracy at two-fold error of prediction was 64%.

Statistically significant QSPkR model was generated by including as descriptor pf<sub>u</sub> – the negative logarithm of the unbound fraction of the drug in plasma f<sub>u</sub>. Data for f<sub>u</sub> were available for 152 molecules. The CL values varied between 0.14 and 290 ml/min/kg, and f<sub>u</sub> values were in the range 0.025 – 0.98 with low values for highly bound drugs, and high values – for low binders. This parameter doesn't have a normal distribution, therefore it should be logarithmically transformed. For better evaluation of

the effect of PPB, it is better to use pf<sub>u</sub> instead of logf<sub>u</sub>, hence high pf<sub>u</sub> value means high PPB.

The dataset was divided into a training set and external test set as described in **Methods**. Six drugs were identified as outliers and were removed before the generation of the final QSPkR, given as Model 2: - **PLEASE SEE BELOW for Model 2**

The model was validated with an external test set of 30 molecules. The statistics on the test set was: r<sup>2</sup><sub>pred</sub> 0.357, GMFEP 1.75 and accuracy 63% (at two-fold error level) and 83% (at 3-fold error level). Three drugs were considered as outliers. The plot of the predicted versus observed values of logCL for the test set is presented in Figure 2.

In addition to plasma protein binding (pf<sub>u</sub>), three types of molecular descriptors emerged in the model: molecular properties (logD<sub>7.4</sub>), E-state indices (H<sub>min</sub>, H<sub>max</sub>, SH<sub>ssNH</sub>, S<sub>ssO</sub> and S<sub>ssCl</sub>) and connectivity indices (xch6). logD<sub>7.4</sub> represents the distribution coefficient at pH 7.4. H<sub>min</sub> and H<sub>max</sub> correspond to the minimum and the maximum hydrogen E-state value in the molecule. SH<sub>ssNH</sub> accounts for the sum of the E-state values of all hydrogen atoms within NH-groups. S<sub>ssO</sub> and S<sub>ssCl</sub> represent the sum of the E-state values of all ether O-atoms and Cl-atoms, respectively, and xch6 is the 6-order chain connectivity index.

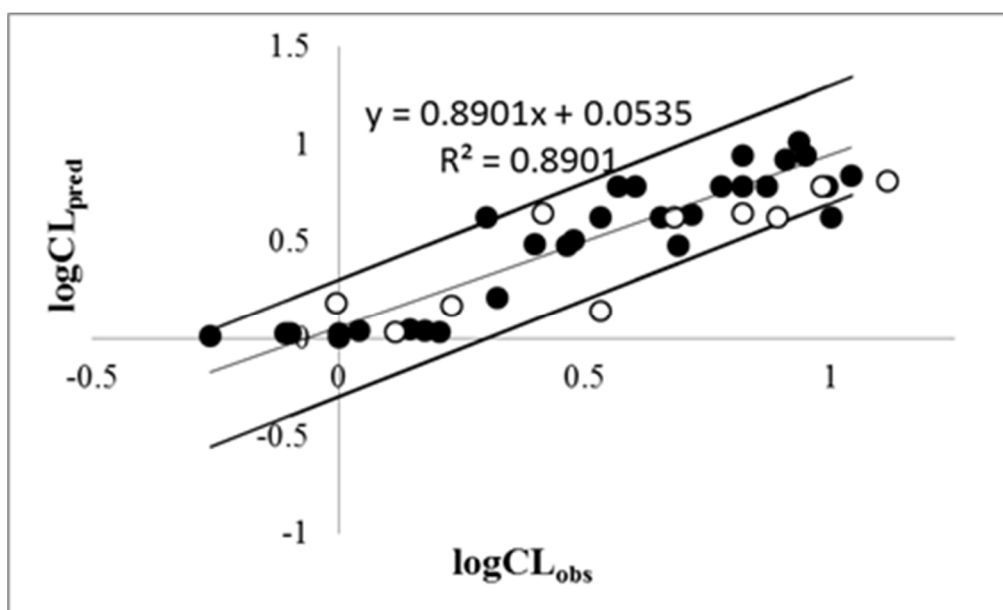


**Figure 1.** Predicted vs. observed logCL values for renally cleared drugs. (●) – training set; (○) – external test set. The straight lines correspond to the regression line for the training set and the two-fold error limits.

**Model 2.**

$$\log CL = -0.273(\pm 0.050)pf_u + 0.120(\pm 0.217)H_{\min} + 0.204(\pm 0.055)H_{\max} + 0.074(\pm 0.022)\log D_{7.4} - 0.073(\pm 0.020)SH_{\text{ssNH}} - 0.026(\pm 0.005)S_{\text{ssO}} - 0.051(\pm 0.011)S_{\text{ssCl}} - 0.801(\pm 0.416)x_{\text{ch6}} + 0.368$$

$n$  116       $r^2$  0.619       $q^2_{\text{Loo-cv}}$  0.531       $F$  17.87

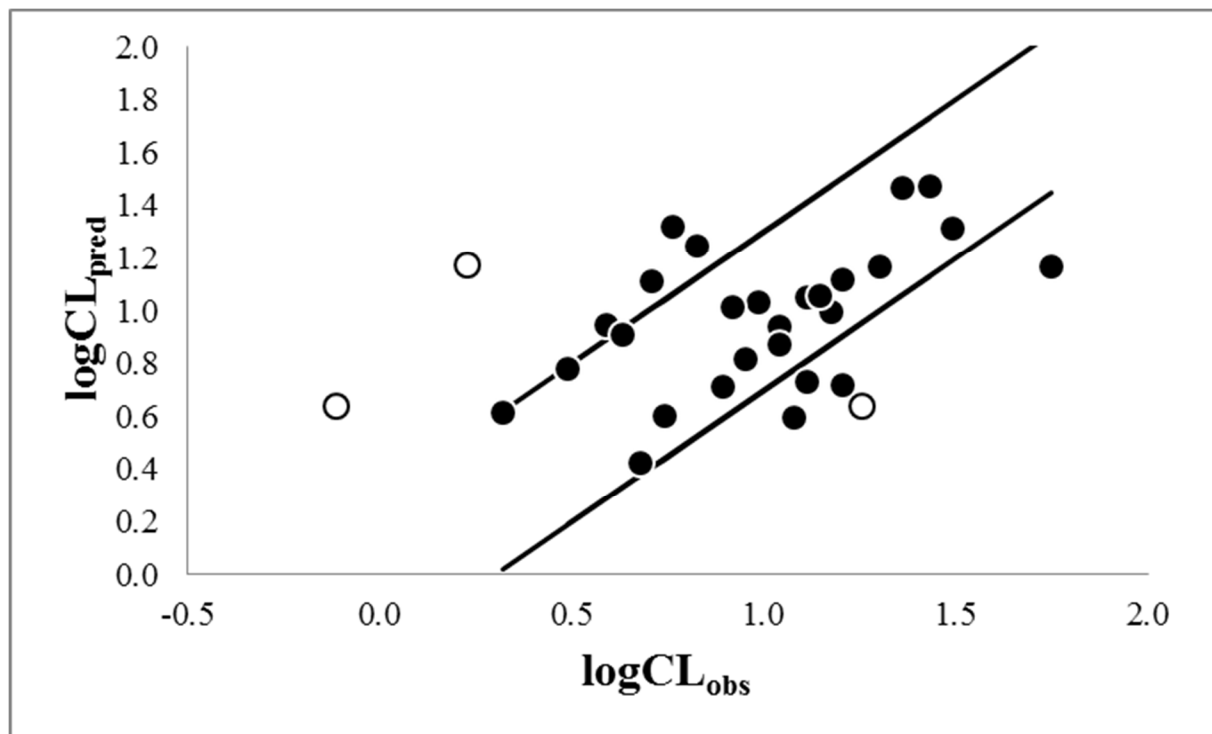


**Figure 2.** Predicted vs. observed  $\log CL$  values in the external test set of drugs, cleared primarily by metabolism. Outliers are presented with blank circles. The straight line corresponds to two-fold error limits.

**QSPkR for drugs, substrates of CYP3A4**

A sound QSPkR model was developed on a dataset of compounds, metabolized solely by CYP3A4 (Model 3):

**Model 3.**

$$\log CL = 44.62(\pm 9.85)x_{\text{vch10}} - 0.126(\pm 0.029)S_{\text{ssO\_acct}} - 2.077(\pm 0.502)x_{\text{ch6}} + 1.008(\pm 0.267)MaxQ_p + 1.104$$

$n$  27       $r^2$  0.668       $q^2_{\text{Loo-cv}}$  0.541      GMFE 1.39      Accuracy(2-fold level): 85%

$X_{\text{vch10}}$  represents the valence 10-order chain connectivity index,  $MaxQ_p$  – the maximum partial positive charge in the molecule,  $x_{\text{ch6}}$  – the 6<sup>th</sup> order chain connectivity index, and  $S_{\text{ssO\_acct}}$  is the sum of all -O-atoms in the molecule.  $pf_u$  was not used as a descriptor for the modeling the CL of drugs, substrates of CYP3A4 because of the lack of data for  $f_u$  of many drugs. However, the restrictive effect of PPB on the CL is discussed in the **Discussion** section.

The model was tested on 60 molecules – substrates of both CYP3A4 and other enzymes. A GMFEP value of 2.21 and accuracy 52% (at two-fold error level) and 75% (three-fold error level) were observed. Eight drugs with a FE > 4 were considered as outliers. Their removal led to a decrease of the GMFEP to 1.91. The plot of the predicted by the model versus observed values of  $\log CL$  is presented in Figure 3.

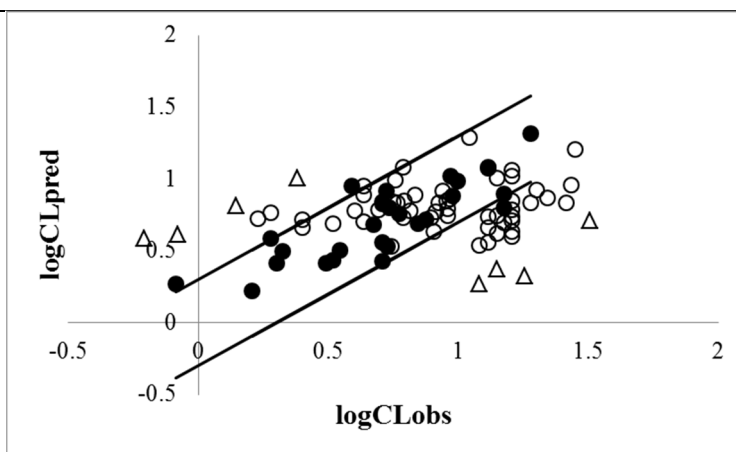


**Figure 3.** Predicted vs. observed logCL data for CYP3A4 substrates. (●) – training set; (○) – drugs predicted with FE < 4; (Δ) – outliers. The straight lines represent the two-fold error limits.

#### QSPkR model for $CL_u$

The dataset of 220 molecules with available data for  $f_u$  was divided into a training set and external test set as described in **Methods**. Seven drugs were

identified as outliers and were removed before construction of the final QSPkR model (Model 4):

#### Model 4.

$$\log CL_u = 0.137(\pm 0.017)\log D_{7.4} + 0.059(\pm 0.014)\text{SaaCH\_acnt} - 0.019(\pm 0.004)\text{ncirc} + 51.86(\pm 11.86)\text{xvch10} + 1.131$$

n 169                       $r^2$  0.552                       $q^2_{\text{LOO-CV}}$  0.522                      F 50.45

Beside  $\log D_{7.4}$ , the value of  $CL_u$  is determined by three structural descriptors: SaaCH\_acnt (the number of non-substituted aromatic C-atoms in the molecule), xvch10 (the 10<sup>th</sup> order connectivity valence index) and ncirc (the number of circles in the molecule). The model was validated on the external

test set (n 44) and showed  $r^2_{\text{pred}}$  0.544 and GMFEP 2.0. 58% and 70% of the drugs were predicted within the two- and three-fold error of observed values. The plot of the predicted by Model 4 versus observed values of  $\log CL_u$  is presented in Figure 4.

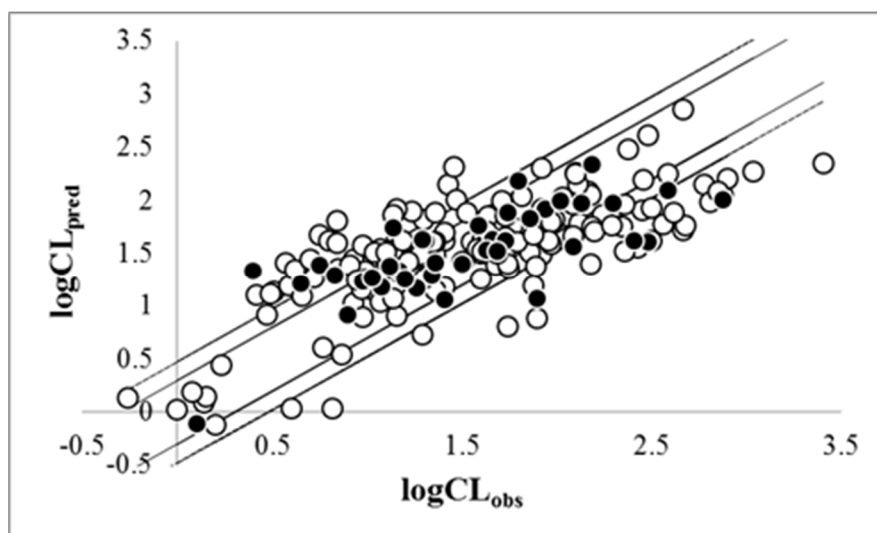


**Figure 4.** Predicted vs. observed  $\log CL_u$  data for the training set (○) and test set (●). The straight lines correspond to the two-fold and three-fold error limits.

## DISCUSSION

The present study presents a number of QSPkR models for the total plasma CL of basic drugs. The whole dataset involved 263 drugs covering wide chemical and biological space. The chemical structures were described by 154 molecular descriptors. The end-point variable was presented as logCL or logCL<sub>u</sub> in order to achieve close to normal distribution. GA, SWR and MLR were used for variable selection and QSPkR models development.

### QSPkR model for renally excreted drugs (Model 1)

Highly significant and predictive model with  $r^2$  0.89 and  $q^2_{\text{LOO-CV}}$  0.85 was developed for the basic drugs, eliminated primarily by renal excretion. The model was able to predict the CL of drugs from an external test set with  $r^2_{\text{pred}}$  0.73, GMFEP 1.57 and accuracy 80% (at two-fold error level) and 100% (at three-fold error level). According to the model, the presence of ether O-atoms affects negatively drug CL, while the presence of three-valence N-atoms (>N- and =N-) has a positive impact.

Analysis of the dataset allowed defining criteria for distinguishing between low- and high CL drugs. Drugs with CL  $\leq$  1.7 ml/min/kg (the value of GFR, 120 mL/min) were assigned as low CL drugs, while drugs with CL  $\geq$  6 ml/min/kg – as high CL drugs. All low CL drugs contained three or four ether O-atoms,

The failure to generate a sound QSPkR on the whole data set of basic drugs directed the research in two ways: deriving QSPkRs for logCL with respect to the primary clearance pathway, and deriving QSPkRs for logCL<sub>u</sub>. Four significant QSPkRs were built: for the CL of drugs, eliminated primarily through renal excretion (Model 1), for drugs with preponderant metabolism (Model 2), for CYP3A4 substrates (Model 3), and for CL<sub>u</sub> of all drugs with available data for  $f_u$  (Model 4).

and no-one involved neither >N-, nor =N-. Conversely, from the high CL drugs, no one had more than one ether O-atom, while 12 compounds contained either >N- or =N-. Therefore, the presence of more than two ether O-atoms was defined as a negative criterion, and the presence of >N- or =N-atom in the molecule – as a positive criterion. Drugs with only negative criteria are expected to have low CL, drugs with only positive criterion – high CL, and drugs with neither positive nor negative criteria – moderate CL. This empirical rule allowed classifying the studied drugs with accuracy of 100% for low CL drugs, 86% – for high CL drugs, and 57% – for moderate CL drugs (Table 1). 20% of the high clearance drugs were incorrectly identified as moderate CL drugs. Respectively, 36% of the moderate CL drugs were incorrectly identified as high clearance drugs and 7% – as low CL drugs. No one low CL drug was classified erroneously.

**Table 1.** Criteria for discrimination between low and high renal CL drugs.

	Clearance, ml/min	Number of ether O-atoms	Number of >N- or =N-	Prediction accuracy, %
Low	$\leq$ 120	$>$ 2	0	100
Moderate	120 - 420	$<$ 2	0	57
High	$\geq$ 420	$<$ 2	$>$ 1	86

### QSPkR model for drugs, cleared primarily by metabolism (Model 2)

The model has fairly good statistics with  $r^2$  0.62 and  $q^2_{\text{LOO-CV}}$  0.53. Although the low value of  $r^2_{\text{pred}}$  for the external test set, Model 2 was able to predict the CL values of the drugs with GMFEP 1.75 and accuracy of 63% (at two-fold error level) and 83% (at 3-fold error level).

Eight descriptors proved to be important for the CL of drugs, eliminated by metabolism. logD<sub>7.4</sub>, the distribution coefficient at pH 7.4, accounts for drug's lipophilicity, and favors drug CL. This is in

agreement with the generally accepted belief that lipophilic drugs are cleared primarily by metabolism (28). However, the contribution of lipophilicity is not unambiguous since drugs with very different logD<sub>7.4</sub> have similar CL, and *vice versa*. For example, reboxetine (CL 0.82 ml/min/kg) and ibutilide (CL 26 ml/min/kg) have logD<sub>7.4</sub> of about 1.8. Thus, lipophilicity is important but not the only determinant of drug CL. H<sub>min</sub> and H<sub>max</sub> (the minimum and the maximum hydrogen E-state value in the molecule) also affect positively drug CL. H<sub>max</sub> encodes the most polar H-atom and has maximum

values for molecules containing OH-groups. The presence of OH-group is a prerequisite for Phase II metabolism. For example, glucuronic acid conjugation is the major metabolism pathway for many high CL drugs like labetalol (29), morphine (30), naloxone (31), etc. Other drugs like fenoterol (32) and R-apomorphine (33) are subjected of both glucuronidation and sulfation. All mentioned drugs possess at least two OH-groups and indeed have high CL values in the range 23 – 40 ml/min/kg.  $H_{\min}$  signifies the less polar H-atom in the molecule and has maximum values for molecules with aromatic rings. The presence of aromatic ring system is a prerequisite for aromatic hydroxylation – one of the most common Phase I metabolic reactions. The highest value of  $H_{\min}$  is observed for triamterene which undergoes extensive oxidative metabolism to p-OH-triamterene (34) and has extremely high CL of 63 ml/min/kg.

PPB is unfavorable for the CL of metabolically cleared drugs. About 55% of the low CL drugs have high PPB ( $f_u < 0.1$ ), while 74% of the high CL drugs have low or moderate PPB ( $f_u > 0.1$ ). As low CL drugs were considered drugs with  $CL < 6$  ml/min/kg (30% of the hepatic blood flow  $Q_H$ ), and as high CL drugs – these with  $CL > 13$  ml/min/kg (70% of  $Q_H$ ). The descriptors SHssNH, SssO, SsCl and xch6 encode the presence, count and electron accessibility of NH-groups, ether O-atoms, Cl-atoms and six-member rings, respectively. The presence of these structural features affects negatively drug CL. Ether O-atoms and secondary amines are potential hydrogen bond acceptors (HBAs). Hydrogen binding ability contributes negatively to lipophilicity, and it was recently reported that the presence of HBAs has a negative effect on drug CL (11).

The presence of Cl-atoms increases metabolic stability by preventing aromatic hydroxylation and glucuronidation of phenols (35). Almost all molecules contain 6-member cycles. In general, the presence of phenyl rings is a prerequisite for aromatic hydroxylation. However, a large number of 6-member rings seem to disfavor drug CL. Most of the drugs with more than three 6-member rings are either extended molecules with molecular weight exceeding 450 g/mol (aripiprazole, doxazosin, imatinib, itraconazole), or contain a number of fused rings (amsacrine, quinine, dihydroquinidine, vincristine). All of them have low CL values (between 0.83 and 5.1 ml/min/kg), most probably due

to steric hindrances by the transport in clearing organs.

Six drugs were identified as outliers from Model 2. Esmolol has extremely high CL of 290 ml/min/kg and it was highly under-predicted by the model. This may be due to its unique metabolism through rapid hydrolysis by red blood cell esterases (36). Oxycodone seems to be over-predicted by the model (CL 6.1 ml/min/kg,  $CL_{\text{pred}}$  19.77 ml/min/kg). However our inspection in the literature found CL values of 0.78 L/min (11.14 ml/min/kg) (37) and 0.83L/min (11.86 ml/min/kg) (38) which are closer to our prediction. Itraconazole is highly under-predicted (CL 5.1 ml/min/kg,  $CL_{\text{pred}}$  0.34 ml/min/kg). The drug exists as a mixture of four cis- and four trans-stereoisomers, most of them substrates and potent inhibitors of CYP3A4, and display stereoselective metabolism to different products (39). These unusual metabolic patterns may be the reason for the inconsistency with the model. Amlodipine is also under-predicted (CL 7 ml/min/kg,  $CL_{\text{pred}}$  1.43 ml/min/kg) which may be due to its very high PPB ( $f_u$  0.005). According to Zhu et al. (40) the drug is slowly cleared primarily via dehydrogenation of its dihydropyridine moiety to a pyridine derivative. Quinine (CL 1.9 ml/min/kg,  $CL_{\text{pred}}$  17.09 ml/min/kg) and terodoline (CL 1.1 ml/min/kg,  $CL_{\text{pred}}$  6.20 ml/min/kg) are also over-predicted. They are low CL drugs, and most probably their molecules contain any negative features not captured by Model 2.

### QSPkR model for drugs, substrates of CYP3A4 (Model 3)

According literature data, 117 drugs in the dataset were metabolized primarily by CytP450 iso-enzymes and 24 – by non-CytP450 pathways (glucuronide, glutathione or sulphate conjugation, hydrolysis, MAO, non-enzymatic processes, etc.). Most of the drugs were substrates of more than one CytP450 or non-CytP450 enzymes. No information was available for the metabolic fate of the rest 29 drugs. We failed to derive QSPkR models for the CL of all CytP-450 substrates ( $n = 117$ ), CYP3A4 (and other enzymes) substrates ( $n = 87$ ) and CYP2D6 (and other enzymes) substrates ( $n = 60$ ). The only significant QSPkR model was built on a small database of drugs, metabolized solely by CYP3A4. The model revealed good statistics on the training set ( $r^2$  0.67, GMFE 1.39). Because of the limited number of compounds, it was assessed only by internal cross-validation ( $q^2_{\text{LOO-cv}}$  0.52).

Four descriptors are important for the CL of CYP3A4 substrates. Xvch10 and MaxQ<sub>p</sub> contribute positively to drug CL. Xvch10 encodes information about the type and substitution patterns in a ring system with 10 edges. It presents in 11 molecules as fused hexagonal rings. For the low CL drugs it is either missing or has a low value. The value of xvch10 is lower for aromatic rings, especially these containing O- or N-atoms, and higher for aliphatic ring systems. The presence of a large hydrophobic center seems to be favorable for the CL which is in agreement with the proposed pharmacophore for CYP3A4 substrates (41). The maximum partial positive charge in the molecule (MaxQ<sub>p</sub>) is usually located at alkyl group, connected with strong electro-negative atom (N- or O-). These moieties are susceptible to O- or N-dealkylation, one of the commonest CYP3A4 catalyzed reactions. All high CL drugs have high MaxQ<sub>p</sub> values, and indeed N-dealkylation is a major metabolic pathway for buprenorphine (42) and propoxyphene (43). A negative effect of xch6 on the CL of drugs cleared mainly by metabolism (Model 2) has already been found and discussed in terms of steric hindrances. Similarly, a high number of ether O-atoms (encoded by SssO\_acnt), which are potential HBAs, may be unfavorable for drug intake in the liver.

It is noteworthy that the analyzed CYP3A4 substrates have relatively low CL and high PPB. There are 18 low CL drugs (< 6 ml/min/kg), 4 high CL drugs (>13 ml/min/kg) and 5 with moderate CL (6 < CL < 13 ml/min/kg). Of the 22 drugs with available f<sub>u</sub> value, 14 have high PPB (f<sub>u</sub> < 0.1) and 8 – moderate PPB (f<sub>u</sub> < 0.4). Thus, high PPB may be typical for CYP3A4 substrates. 62% of the low CL drugs have high PPB, which seems to be restrictive factor for elimination. In contrast, buprenorphine, ergothamine, saquinavir and propoxyphene demonstrate rather high CL despite of their high PPB. Obviously, their intrinsic clearance is high enough to overcome PPB.

Model 3 was tested on 60 molecules – substrates of both CYP3A4 and other enzymes. Fairly good predictive ability was observed as proved by GMFEP and accuracy. Most of the drugs were under-predicted which was not surprising as CYP3A4 metabolism represented only a part of the total elimination pathway. Four outliers from the model (cocaine, gefitinib, telithromycin and verapamil) were highly under-predicted with FE > 4. The major metabolic pathways for cocaine are catalyzed by esterases in plasma and tissues, while

CYP3A4 mediated demethylation is only a minor route (44). Gefitinib is mainly metabolized in the liver by cytochrome CYP3A4, CYP3A5 and CYP2D6. The main metabolic pathway characterized by using human liver microsomes include morpholine ring opening, O-demethylation of the methoxy-substituent on the quinazoline ring structure and oxidative defluorination of the halogenated phenyl group (45). Telithromycin is eliminated by multiple pathways – biliary and/or intestinal excretion (7%), renal excretion (13%) and hepatic metabolism via CYP 3A4 and non-CytP-450 pathways (46). Trazodone undergoes extensive hepatic metabolism via hydroxylation, N-dealkylation, N-oxidation and splitting of the pyridine ring, catalyzed by CYP3A4 and CYP2D6 (47). In contrast, aripiprazole, azimilide, tamsulosin and trazodone were highly over-predicted. Although these molecules contain favorable structural features, their CL seems to be restricted by the high PPB (f<sub>u</sub> 0.01 – 06).

#### QSPkR model for CL<sub>u</sub> (Model 4)

CL<sub>u</sub> is the clearance of the unbound drug in plasma. It is considered as independent of PPB and determined solely by the molecular structure. However, it is calculated from two experimental variables which increases the risk of uncertainty of the modeled parameter. In general, the generated QSPkR meets the statistical criteria for well predictive models, however the GMFEP is at the upper allowed limit and accuracy is lower. Nevertheless the model reveals structural features important for CL<sub>u</sub> of basic drugs.

The most significant determinant for CL<sub>u</sub> is logD<sub>7.4</sub> which accounts for nearly 40% of the explained variance. The positive effect of logD<sub>7.4</sub> is reasonable as lipophilicity is of paramount importance for many processes involved in drug elimination (uptake in the elimination organs, interaction with the binding site, etc.). For 78% of the 50 drugs with the lowest CL<sub>u</sub> values logD<sub>7.4</sub> < 1, and almost half of them are eliminated primarily by renal excretion. On contrary, 74% of the 50 drugs with the highest CL<sub>u</sub> values have logD<sub>7.4</sub> > 2 and all of them are subjected to extensive metabolism. The presence of non-substituted aromatic C-atoms in the molecule, encoded by SaaCH\_acnt, also contributes positively to CL<sub>u</sub>. These atoms are potential sites of aromatic hydroxylation – one of the most abundant paths of oxidative metabolism. 84% of the high CL<sub>u</sub> drugs contain more than 5 aromatic CH- groups,

while this number is less than 25% for the low  $CL_u$  compounds. The 10<sup>th</sup> order connectivity valence index  $xvch_{10}$  encodes the number and substitution patterns of a ring system with 10 edges (in the current database – fused hexagonal rings, or 7- and 5-member rings). As previously shown,  $xvch_{10}$  affects positively the CL of CYP3A4 substrates. This could be explained with the requirement for large hydrophobic centers in the drug molecule able to fit in the enzyme active sites.  $ncirc$  accounts for the number of circles in the molecule. Most of the drugs with large number of circles ( $> 15$ ) have high

molecular weight, volume and surface. The negative impact of this descriptor could be due to steric hindrances for the uptake in the clearance organs.

Twelve drugs (with residuals  $>1$ ) were identified as outliers from the model: 7 – from the training set, and 5 – from the test set. They are presented in Table 1 together with data for their CL,  $f_u$ ,  $CL_u$  and  $\log D_{7.4}$ .

The first eight drugs are highly under-predicted. Most of them have low to moderate CL, but extremely high PPB (exceeding 98%), which results in enormous and unrealistic high values of  $CL_u$ .

**Table 1.** Outliers from the QSPkR model for  $CL_u$  of basic drugs.

Drug	CL, ml/min/kg	$f_u$	$CL_u$ , ml/min/kg		$\log D_{7.4}$
			observed	predicted	
Amiodarone	1.9	0.0002	9,550	228	6.94
Amlodipine	7	0.005	1,413	49	2.64
Amsalog	2.6	0.0011	2,344	71	1.33
Esmolol	290	0.59	488	23	0.06
Hydralazine	85	0.12	708	31	0.28
Oxybutynin	5.1	0.0034	1,513	94	4.29
Tegaserod	18	0.02	891	43	2.39
Ziprasidone	5.1	0.0012	4,266	59	3.07
Cetorelix	1.2	0.14	8.5	226	0.69
Chlorpheniramine	2.5	0.70	3.6	55	1.29
Methadone	1.7	0.21	8	108	2.56
Pyrimethamine	0.052	0.1	0.55	49	2.66

Esmolol and hydralazine are the drugs with the highest CL values in the dataset. Their inconsistency with the model may be due to their low lipophilicity which is, according to Model 4, the most significant determinant of  $CL_u$ . The other four drugs are over-predicted. They are low CL drugs with moderate or low PPB. Most probably they contain any unfavorable structural features which are not captured by the model. Furthermore, cetorelix is a drug with a very large molecular weight (1431 g/mol) and low lipophilicity, and the lower observed value of  $CL_u$  may be due to hindered transport in the clearing organs.

## CONCLUSIONS

The study presents a number of significant, predictive and interpretable QSPkR models for the CL of basic drugs. Separate models were generated for the CL of drugs according to their primary elimination pathway – renal excretion, metabolism, or CYP3A4 mediated metabolism, as well as for the unbound clearance  $CL_u$  depending on PPB. The

models allow prediction of 52 – 80% of the drugs from external validation sets within the 2-fold error of experimental values. The descriptors in the models reveal clear structural features determining the CL of basic drugs. The major factor disfavoring drug CL (particularly for drugs eliminated primarily by metabolism) is PPB. The most important (but not the only) factor with a positive effect on drug CL is lipophilicity, expressed as  $\log D_{7.4}$ . The clearance of metabolically cleared drugs is further favored by the presence of OH-groups, aromatic rings, large hydrophobic centers, aliphatic groups, bonded to electro-negative atoms, and non-substituted aromatic C-atoms. The presence of Cl-atoms, large number of 6-member aromatic rings or fused rings disfavors drug CL. The CL of both renal and metabolism cleared drugs are negatively affected by ether O-atoms, and urine excretion is favored by the presence of 3-valence N-atoms ( $-N=$  or  $>N-$ ). These findings give insight on the main structural features governing the CL of basic drugs and could serve as a guide for lead optimization in the drug development process.

## REFERENCES

1. Kola I, Landis J. Can the pharmaceutical industry reduce attrition rates? *Nature Rev/Drug Discov*, 2004; 3:711-715.
2. Van der Waterbeemd H, Gifford E. ADMET in silico modeling: towards prediction paradise? *Nature*, 2003; 2:192-204.
3. Yamashita F, Hashida M. In silico approaches for predicting ADME properties of drugs. *Drug Metab Pharmacokin*, 2004; 19(5):327-337.
4. Mager DE. Quantitative structure – pharmacokinetic/pharmacodynamics relationships. *Adv Drug Deliv*, 2006; 58:1326-1356.
5. Chihan KK, Paine SW, Waters NJ. Advancements in predictive in silico models for ADME. *Cur Chem Biol*, 2008; 2:215-228.
6. Madden JC. Ch. 10. In silico approaches for predicting ADME properties, in Pyzyn T; Leszczynski J; Cronin MTD (eds), *Recent advances in QSAR studies*, Springer, Dordrecht, Heidelberg, London, New York, pp. 283-304, 2010.
7. Toutain PL, Bousquet-Melou A. Plasma clearance. *J Vet Pharmacol Therap*, 2004; 27:415-425.
8. Karalis V, Tsantali-Kakoulidou A, Macheras P. Quantitative structure – pharmacokinetic relationships for disposition parameters of cephalosporins. *Eur J Pharm Sci* 2003; 20:115-123.
9. Ng C, Xiao Y, Putnam W, Lum B, Tropsha A. Quantitative structure – pharmacokinetic parameter relationships (QSPkR) analysis of antimicrobial agents in human using simulated k-nearest neighbor and partial least square analysis methods. *J Pharm Sci*, 2004; 93:2535-2544.
10. Yap CW, Li ZR, Chen YZ. Quantitative structure – pharmacokinetic relationships for drug clearance by using statistical learning methods. *J MNol Graph Model*, 2006; 24:383-395.
11. Berellini G, Waters NJ, Lombardo F. In silico prediction of total plasma clearance. *J Chem Inf Model*, 2012; 52:2069-2078.
12. Lombardo F, Obach RS, Varma MV, Stringer R, Berellimmi G. Clearance mechanism assignment and total clearance prediction in human based upon in silico models. *J Med Chem*, 2014; 57:4392-4405.
13. Turner JV, Maddalena DJ, Cutler DJ, Agatonovic – Kustrin S. Multiple pharmacokinetic parameter prediction for a series of cephalosporines. *J Pharm Sci*, 2003; 92:552-559.
14. Yu MJ. Predicting total clearance in humans from chemical structure. *J Chem Inf Model*, 2010; 50:1284-1295.
15. Smith DA, Allerton C, Kalgutkar AS, Waterbeemd H, Walker DK. Distribution, in Smith DA; Allerton C; Kalgutkar AS; Waterbeemd H; Walker DK (eds), *Pharmacokinetics and metabolism in drug design*, 3rd ed, Weinheim, Wiley – VCH Verlag GmbH&Co. KgaA, pp. 61-79, 2012.
16. Pelis RM, Wright SH. Renal transport of organic anions and cations. *Compr Physiol*, 2011; 1:1795-1835.
17. Kusama M, Toshimoto K, Maeda K, Hirai Y, Imai S, Chiba K, Akiyama Y, Sugiyama Y. In silico classification of major clearance pathways of drugs with their physicochemical properties. *Drug Metab Dispos*, 2010; 38(8):1362-1369.
18. Zhivkova Z, Doytchinova I. Prediction of steady-state volume of distribution of acidic drugs by quantitative structure-pharmacokinetics relationships. *J Pharm Sci*, 2012; 101(3):1253-1266.
19. Zhivkova Z, Doytchinova I. Quantitative structure – plasma protein binding relationships of acidic drugs. *J Pharm Sci*, 2012; 101(12):4627-4641.
20. Zhivkova Z, Doytchinova I. Quantitative structure – clearance relationships of acidic drugs. *Mol Pharmac*, 2013; 10:3758-3768.
21. Zhivkova Z, Doytchinova I. In silico quantitative structure – pharmacokinetic relationship modeling on acidic drugs: half-life. *Int J Ohrm Pharm Sci*, 2014; 6(9):283-289.
22. Zhivkova Z, Doytchinova I. Quantitative structure – pharmacokinetic relationships analysis of basic drugs: Volume of distribution. *J Pharm Pharm Sci*, 2015; 18(3):515-527.
23. Obach RS, Lombardo F, Waters NJ. Trend analysis of a database of intravenous pharmacokinetic parameters in humans for 670 drug compounds. *Drug Metab Dispos*, 2008; 36(7):1385-1405.
24. <https://www.drugbank.ca/>
25. <http://www.chemicalbook.com/>
26. <http://www.nikkajiweb.jst.go.jp/>
27. Roy K, Kar S, Das RN, Statistical methods in QSAR/QSPR, in Roy K; Kar S; Das RN (eds), *A primer on QSAR/QSPR modeling*. Fundamental concepts, Springer Cham, Heidelberg, New York, Dordrechts, London, pp 37-59, 2015.
28. Benet LZ, Broccateli F, Oprea TI. BDDCS applied to over 900 drugs. *The APPS Journal*, 2011; 12(4):511-547.
29. McNeil JJ, Louis WJ. Clinical pharmacokinetics of labetalol. *Clin Pharmacokinet*, 1984; 9(2):157-167.
30. Glare PA, Walsh TD. Clinical pharmacokinetics of morphine. *Ther Drug Monit*, 1991; 13(1):1-23.
31. Wahlstrom A, Persson K, Rane A. Metabolic interaction between morphine and naloxone in human liver. A common pathway of glucuronidation? *Drug Metab Dispos*, 1989; 17(2): 218-220.
32. Hildebrandt R, Wagner B, Preiss – Nowzohour K, Gundert – Remy U. Fenoterol metabolism in man: sulphation versus glucuronidation. *Xenobiotica*, 1994; 24(1):71-77.
33. Van der Geest R, Kruger P, Gubbens-Stibbe JM, Van Laar T, Bodde HE, Danhof M. Assay of R-

- apomorphine, S-apomorphine, apocodeine, isoapocodeine and their glucuronide and sulphate conjugates in plasma and urine of patients with Parkinson's disease. *J Chrom B: Biomed Sci Appl*, 1997; 702(1-2): 131-141.
34. Gilfich HJ, Kremer G, Moerke W, Mutschler E, Voelger KD. Pharmacokinetics of triamterene after iv administration to man: determination of bioavailability. *Eur J Clin Pharmacol*, 1983; 25(2): 237-241.
  35. Kerns EH; Di L, Drug-like properties: concepts, structure design and methods. 2<sup>nd</sup> ed., Elsevier, Amsterdam, Boston, Heidelberg, etc, pp. 161-197, 2016.
  36. Reynolds RD, Goczynsky RJ, Quon CY. Pharmacology and pharmacokinetics of esmolol. *J Clin Pharmacol*, 1986; 26, Suppl. A: A3-A14.
  37. Pouhia R, Seppala T, Olkkola KT, Kaslo E. The pharmacokinetics and metabolism of oxycodone after intramuscular and oral administration in healthy subjects. *Br J Clin Pharmacol*, 1992; 33: 617-621.
  38. Takala A, Kaasalainen V, Seppala T, Kaslo E, Olkkola KT. Pharmacokinetic comparison of intravenous and intranasal administration of oxycodone. *Acta Anaesthesiol Scand*, 1997; 41(20):309-312.
  39. Peng C-C, Shi W, Lutz JD, Kunze KL, Liu JO, Nelson WL, Isoherranen N. Stereoselective metabolism of itraconazole by CYP3A4: dioxolane ring scission of azole antifungals. *Drug Metab Dispos*, 2012; 40(3): 426-435.
  40. Zhu Y, Wang F, Li Q, Du, A, Tang, W, Chen, W. Amlodipine metabolism in human liver microsomes and roles of CYP3A4/5 in the dihydropyridine dehydrogenation. *Drug Metab Dispos*, 2014; 42(2): 245-249.
  41. Ekins S, Bravi G, Wikel JH, Wrighton SA. Three-dimensional quantitative structure – activity relationship analysis of Cytochrome P-450 3A4 substrates. *J Pharmacol Exp Ther* 1999, 29(1): 424-433.
  42. Elkader A, Sproule B. Buprenirphine: clinical pharmacokinetics in the treatment of opioid dependence. *Clin Pharmacokinet*, 2005; 44(7):661-680.
  43. Due SL, Sullivan HR, McMahon RE. Propoxyphene: pathways of metabolism in man and laboratory animals. *Biomed Mass Spectrom*, 1976; 3(5):217-225.
  44. Kolbrich EA, Barnes AJ, Gorelick DA, Boyd SJ, Cone EJ, Hiesfis MA. Major and minor metabolites of cocaine in human plasma following controlled subcutaneous cocaine administration. *J Anal Toxicol*, 2006; 30:501-510.
  45. Alfieri R, Galetti M, Tramonti S, Andreoli P, et al. Metabolism of the EGFR tyrosin kinase inhibitor gefitinib by cytochrome P450 1A1 enzyme in EGFR-wild type non small cell lung cancer cell lines. *Mol Cancer*, 2011; 10:143, <http://www.molecularcancer.com/10/1/143>.
  46. Shi J, Montay G, Bhargava VO. Clinical pharmacokinetics of telithromycin, the first ketolide antibacterial. *Clin Pharmacokinet*, 2005; 44(9):915-934.
  47. Golden RN; Dawkins K; Nichilas L, Trazodone and nefazodone, in Scatzberg AF; Nemeroff CB (eds.) *The American psychiatric publishing textbook of psychopharmacology*, 4<sup>th</sup> ed., American Psychiatric Publ Inc, Aelington, VA, 2009.